

ON THE STABILITY OF HYBRID AC-DC MICROGRIDS IN VARIOUS LOADS AND SHORT CIRCUIT FAULTS CONDITIONS

Akbar Dadkhah¹, Navid Bayati¹, Behrooz Vahidi^{1*}, Seyed Hossein Hesamedin Sadeghi¹
 1-Department of Electrical Engineering, Amirkabir University of Technology, Tehran 1591634311, Iran

* Corresponding author email: vahidi@aut.ac.ir

Abstract: Microgrids are small power systems contain distributed energy resources like Photo Voltaic(P.V), Wind, Fuel cell, Micro turbine and energy storage devices such as battery, etc. that will play an important role in future power systems. Individual AC or DC microgrids have been conventional at last decade. Different appliances at the demand side with DC or AC energy usage require multiple reverse conversions (AC/DC or DC/AC).When the number of converters increases cost, intricacy of control and volume of circuits will be multiplied accordingly, and reliability and efficiency of the system will be reduced. To reduce the number of converters a hybrid AC-DC Microgrid is proposed by L. Xiong et al. In the hybrid microgrid both AC and DC networks are connected together and multi bidirectional converters join individual networks. Wind turbine and P.V array act as Distribution Generation (DG) units. Suggested control method by L. Xiong et al can help the system to work stable under different generation and load block usage conditions. In this paper, the suggested method by L. Xiong et al is examined for short circuit fault conditions and reliability of the network will be discussed. Simulation results show that system can operate stable when a fault occurs and stability of the system is improved in comparison with proposed model by A. V. Jayawardena et al.

Keywords: Hybrid Microgrid, DG units, Short circuit, Reliability

1. INTRODUCTION

Many researchers are used different search algorithms and technical software for solving power system problems [1-7]. Energy works as a base of any advance. Looking at existent trends, it is obvious that fossil fuels cannot support the load of rapid industrial and residential growth for longer time. In addition, because of environmental issues such as gas emission, global warming, and increasing costs of energy, governments concentrate on renewable-energy resources. Renewable-energy resources can be an effective alternative to conventional sources. Since solar cell and wind energy are intermittent in nature, their energy production is not certain and predictable. Every time that a new DG unit is added to the system, control of the system will become more sophisticated. Because of this challenges a hybrid network of renewable-energy resources is used in new networks so it can act as a reliable system. In last decade's most electric loads were AC such as heating, ventilating and air conditioning (HVAC) systems, lights and motors. Using more electronics devices such as light-emitting diode (LED), computers, etc. changed the conventional AC system's load to DC load. AC and DC microgrids with distributed energy resources are presented in [8]-[10]. In the AC microgrid for using energy obtained from P.V arrays, fuel cell and battery, DC/AC converters (inverters) should be used and for providing energy for DC loads, AC/DC converters are necessary. In AC or DC microgrids multiple reverse conversions requirement, increases cost and intricacy of the circuit and will reduce the efficiency of the system. In figure1 excessive number of converters in AC or DC microgrids is shown.

In this paper, a hybrid AC-DC microgrid is used [11]. Figure 2 shows a typical hybrid microgrid. Implementation of hybrid microgrid can reduce multiple conversions and hence will decrease cost, energy losses and complexity of the system. A control method for

proposed network under different conditions is tested, short circuit fault and reliability of the system in grid tied and isolated modes will be discussed. AC and DC networks are connected through a bidirectional converter which can work in inverter or rectifier mode. P.V arrays and DC load are connected to the DC network, wind turbine generator and AC load are connected to the AC network.

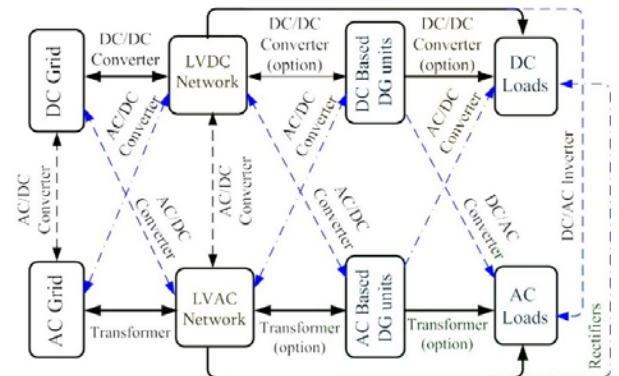


Figure. 1. Excessive number of converters for AC and DC microgrids.

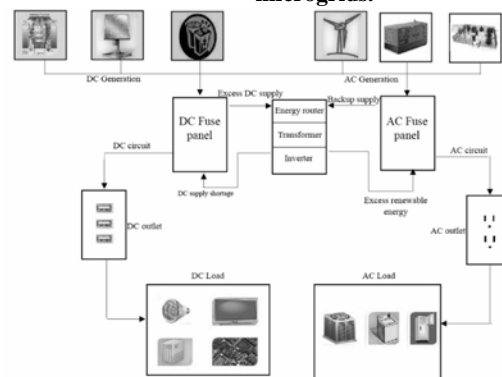


Figure. 2. A typical hybrid AC/DC microgrid.

P.V arrays are connected to the DC load through the switching boost converter. Wind turbine generator (WTG) is connected to the AC load through a doubly fed induction generator (DFIG) that can be controlled in Direct Power Control (DPC) or Direct Torque Control (DTC) [12]. Main converter works in two modes. When the power created by P.V arrays is greater than usage in DC side, extra power is sent to the AC side and the main converter acts as an inverter, and when energy production in DC side is less than load usage, direction of power will be reversed. When the total harnessed energy from WTG and P.V is not enough to supply the loads, utility grid injects the power to the microgrid. For achieving maximum energy both WTG and PV use maximum power point tracking (MPPT) techniques.

2. NETWORK FORMATION

Hybrid AC-DC microgrid is shown in figure 3 [11]. System is made up of an AC and a DC grid on left and right sides respectively. AC side is connected to the main grid by a transformer. P.V arrays are connected to DC grid and WTG is connected to AC grid. PV module is connected to the DC load through a boost converter. WTG is connected to AC load through a DFIG. Model components are presented in table 1 [11]. C_{pv} is used to block high frequency (HF) ripple of the P.V voltage. C_d is enough large to make constant the output voltage of solar cell. Rated value of P.V arrays, battery, WTG, AC and DC loads are represented in table 2 [11]. Battery is connected to the DC side through a bidirectional converter. Battery has an important role only in isolated mode and in the grid tied mode main grid acts for balancing power between DC and AC sides. AC and DC buses are interacting with each other through a bidirectional main converter with an isolating transformer.

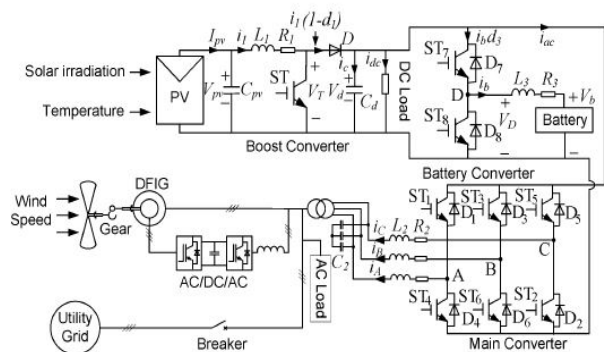


Figure.3. Proposed hybrid AC/DC microgrid used in this paper [11].

3. NETWORK PERFORMANCE

Subjective of the network is to provide a stable DC bus voltage and reliability of the system. MPPT method is used for both P.V arrays and WTG to achieve maximum power. When maximum power of the P.V panels is more than DC load usage, main converter acts as an inverter. If

the total consumption of AC and DC loads is smaller than produced power of renewable-energy resources remaining needed power will be injected to hybrid microgrid from main AC grid. In the grid tied mode excessive power is sent to the AC side and injected to the main grid. If the grid works in isolated mode, extra power is stored in the battery. In this paper, the voltage stability of DC side under various conditions of load and faults that occurred in the grid tied and isolated modes is investigated and results are compared with the result of short circuit fault in [13].

TABLE 1. PARAMETERS OF HYBRID AC-DC MICROGRID [11].

Symbol	Illustration	Value
C_{pv}	Capacitor of PV	110uF
L_1	Inductor of the boost converter	2.5mH
C_d	Capacitor of the DC link	4.7mF
L_2	Inductor of the inverter	0.43mH
R_2	Resistor of the inverter	0.3ohm
C_2	Capacitor of the inverter	60uF
L_3	Inductor of the battery converter	3mH
R_3	Resistance of L3	0.1ohm
F	Main grid frequency	60Hz
F_s	Switching frequency of converters	10kHz
V_d	Rated DC bus voltage	400V
$V_{ll}(rms)$	Rated AC bus voltage	400V
$N_1:N_2$	Transformer ratio	2:1

TABLE 2. NOMINAL POWER OF NETWORK'S COMPONENTS.

Part	Nominal Power/Energy
P.V arrays	40kW
WTG	50kW
Battery	65Ah
AC/ DC load	(20-40)kW

3.1. Modeling WTG

WTG output power is concluded from (1)

$$\frac{1}{2} \rho A C_p(\lambda, \beta) V_\omega^3 \quad (1)$$

ρ is air density, A is rotor swept area, $C_p(\lambda, \beta)$ is power coefficient and V_ω is wind speed. For controlling of DFIG mathematical models (4) and (5) are used that mentioned in [11]. Statements (2) and (3) show dynamic equations of Doubly Fed Induction Generator.

$$\frac{J}{n_p} \frac{d\omega_r}{dt} = T_m - T_{em} \quad (2)$$

$$T_{em} = n_p L_m (i_{qs} i_{dr} - i_{ds} i_{qr}) \quad (3)$$

$$\begin{bmatrix} u_{ds} \\ u_{qs} \\ u_{dr} \\ u_{qr} \end{bmatrix} = \begin{bmatrix} -R_s & 0 & 0 & 0 \\ 0 & -R_s & 0 & 0 \\ 0 & 0 & R_r & 0 \\ 0 & 0 & 0 & R_r \end{bmatrix} \begin{bmatrix} i_{ds} \\ i_{qs} \\ i_{dr} \\ i_{qr} \end{bmatrix}$$

$$+P \begin{bmatrix} \lambda_{ds} \\ \lambda_{qs} \\ \lambda_{dr} \\ \lambda_{qr} \end{bmatrix} + \begin{bmatrix} -\omega_1 \lambda_{qs} \\ \omega_1 \lambda_{ds} \\ -\omega_2 \lambda_{qr} \\ \omega_2 \lambda_{dr} \end{bmatrix} \quad (4)$$

$$\begin{bmatrix} \lambda_{ds} \\ \lambda_{qs} \\ \lambda_{dr} \\ \lambda_{qr} \end{bmatrix} = \begin{bmatrix} -L_s & 0 & L_m & 0 \\ 0 & -L_s & 0 & L_m \\ -L_m & 0 & L_r & 0 \\ 0 & -L_m & 0 & L_r \end{bmatrix} \begin{bmatrix} i_{ds} \\ i_{qs} \\ i_{dr} \\ i_{qr} \end{bmatrix} \quad (5)$$

T_m and T_{em} are mechanical and electromagnetic torque respectively. Remaining parameters of DFIG are shown in table 3 [11].

U is representing the voltage, i is for current, λ is for flux linkage, L is for inductance, d and q symbolize the d-axis and q-axis, r and s represent rotor and stator respectively. Complementary equations are represented in [14], [15].

Formulas (6) and (7) can be used for representing active and reactive power of DFIG:

$$P_s = u_s i_{ds} + u_{qs} i_{qs} \quad (6)$$

$$Q_s = u_{qs} i_{ds} - u_{ds} i_{qs} \quad (7)$$

Voltage equations of (u_{ds} , u_{dr} , u_{qs} and u_{qr}) are brought in [11].

3.2. Modeling PV Array

Model of the P.V cell is shown in figure 4. Parameters of P.V panel are shown in Table 4 [11]. I_{pv} is the output current of solar cell. I_{ph} and I_{sat} given in [16], [17].

$$I_{pv} = n_p I_{ph} - n_p I_{sat} \left[\exp \left(\frac{q}{A k T} \right) \left(\frac{V_{pv}}{n_s + I_{pv} R_s} \right) - 1 \right] \quad (8)$$

Typical MPPT technique to harness maximum power from solar cell can be seen in figure 5 [18], [19].

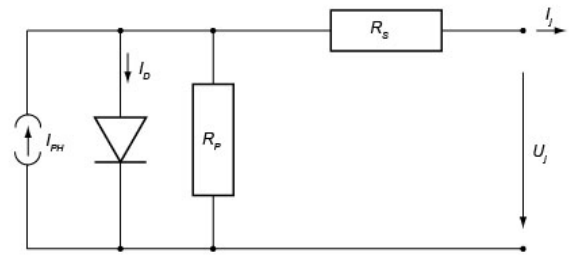


Figure 4. Model of P.V cell.

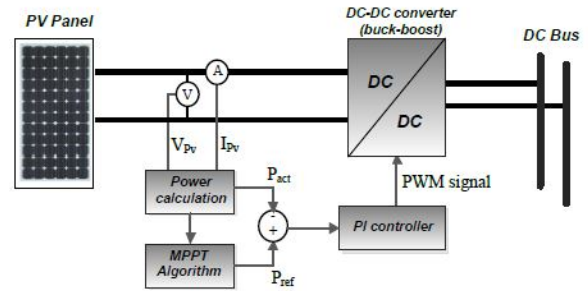


Figure 5. MPPT technique for P.V cell to harness maximum power [18].

TABLE 3.

PARAMETERS OF DFIG [11]

Symbol	Illustration	Value
P_{nom}	Rated power	50kW
V_{nom}	Rated voltage	400V
R_s	Stator resistance	0.00706pu
L_s	Stator inductance	0.171pu
R_r	Rotor resistance	0.005pu
L_r	Rotor inductance	0.156pu
L_m	Mutual inductance	2.9pu
J	Inertial constant	3.1sec
n_p	Number of poles	6
V_{dc}	Rated DC voltage of AC/DC/AC converter	800V
P_m	Rated mechanical power	45kW

4. CONTROL OF CONVERTERS

Five converters exist in this model that should be controlled to improve stability of the system and supply the load correctly.

In the grid tied mode utility grid balances power of the system. With variable loads at DC and AC sides, the main converter should bring in stability of the DC link voltage

toward the faults and load changes and synchronize the AC side with the utility grid.

TABLE 4.
PARAMETERS OF P.V PANEL [11]

Symbol	Illustration	Value
V_{oc}	Nominal open circuit voltage	403V
I_{ph}	Photocurrent	
I_{sat}	Reverse saturation current	
I_{sso}	Short circuit current	3.27A
I_{rr}	Reverse saturation current at Tr	$2.0793e^{-6}A$
E_{gap}	Silicon band gap energy	1.1eV
Q	Electron charge	$1.602 \cdot 10^{-19}C$
R_s	Series resistance of PV cell	
R_p	Parallel resistance of PV cell	
n_s	Number of cells in series	900
n_p	Number of cells in parallel	40
T_r	Reference temperature	301.18K
T	Surface temperature of PV	350K
S	Solar irradiation level	0-1000W/m ²
K	Boltzman constant	$1.38 \cdot 10^{-23}J/K$
K_i	SC current temperature coefficient	$1.7e^{-3}$
A	Ideality factor	1.5

Because of the intermittent nature of wind and solar irradiation, controllers should change their operational modes for better performance of the system. Boost converter should use the MPPT technique for solar cell, and AC/DC/AC converter of DFIG must use the MPPT technique and synchronize the WTG with main AC grid. In this mode battery doesn't have any important role and power is adjusted by main AC grid. Power flow statements of this mode are as bellows [11]:

$$P_{pv} + P_{ac} = P_{dcL} + P_b \quad (9)$$

$$P_s = P_w - P_{acL} - P_{ac} \quad (10)$$

P_{pv} and P_w are real power that came from solar cell and WTG. P_{dcL} and P_{acL} are power usage of loads that are connected to DC and AC sides respectively. P_b is power sent to the battery. P_s is power sent to the main grid from the hybrid system and P_{ac} is power traded between AC and DC sides. Complete formulas are given in [11]. Based on given formulas in [11] the control block diagram for main and boost converters is shown in figure 6.

The outer loop is tracking reference voltage without any error and the inner loop is for enhancing dynamic response. Saturation limiter and delay can improve tracking speed of V_{PV} . A PQ controller can be used in main converter with a current controlled voltage source to obtain a soft exchange power between AC and DC sides. For controlling active and reactive power PI controllers are implemented. With falling in power usage at DC side main converter should work to send extra power from DC to AC grid. If the DC load increased suddenly, power shortage will be taken place and V_d drops at the AC side. So main converter helps the grid to inject power from AC to DC side. Also method of controlling the DFIG is represented in [11]. In this paper, direct torque control method is used for rotor side converter. Isolated mode is also represented in [10].

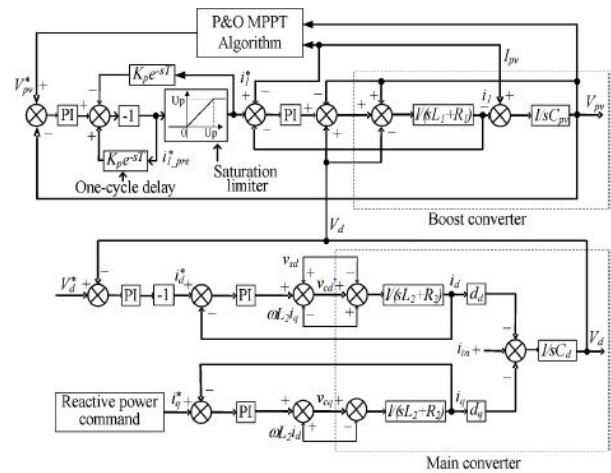


Figure 6. Controller of the main/boost converters [11].

5. SIMULATION RESULTS

Performance of the hybrid AC-DC microgrid is simulated in MATLAB/SIMULINK. Various conditions of loads and renewable-energy sources are considered. Short circuit faults in the grid tied, and isolated modes are occurred and capability of coordination control to increase the reliability of the network is shown in next parts.

5.1. Voltage Stability in the Grid Tied Mode

In the grid tied mode main converter works at PQ mode. DC side voltage is balanced with main converter and AC side voltage is balanced with main grid. Perturbation and observation (P&O) algorithm for tracking solar irradiation is used [19]. Figures 7 and 8 show that P&O algorithm can track changes as fast as irradiation level changes. For different solar irradiation, output voltage and current of solar panel are shown in figure 8. Solar irradiation from 0 to 0.1s is set to 400 W/m², from 0.1s to 0.15s intensifies linearly from 400 W/m² to 1000 W/m², from 0.15s to 0.35s will be constant, from 0.35s to 0.4s declines linearly to 400 W/m² and then remains constant till 0.5s. Solar irradiation changes is shown in figure 7.

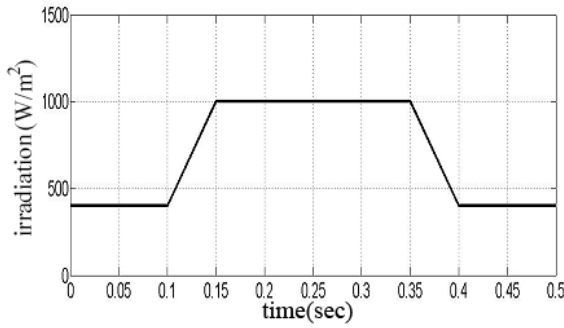


Figure 7. Solar irradiation changes.

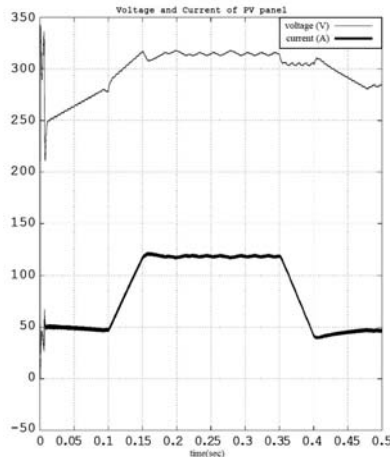


Figure 8. Output current and voltage of solar panel.

Figure 9 shows changes of output power of the solar panel according to changes in solar irradiation. Output power of the P.V arrays is (12.5 kW - 37.5 kW).

In the next part the impact of load changes and short circuit fault on DC bus voltage and effectiveness of the control method represented in [11] are investigated.

When solar irradiation is constantly (750 W/m²), DC load grows from 20kW to 40kW at t = 0.25s. Figure 10 shows voltage response of the DC side of the network. So main converter controller can maintain stable the DC bus voltage. DC bus voltage after increasing DC load is dropped at 0.25sec and as fast as possible the main converter acts, power is injected into the DC grid and DC voltage is recovered.

5.2. Voltage Stability of DC Bus under Short Circuit Fault

For best understanding efficiency of the control method, 3 Phase short circuit faults in isolated and grid tied modes are tested.

If a 3 Phase short circuit faults is applied at the AC side in grid tied and isolated modes it can be observed that proposed controller can bring fast action to guarantee the stability of the DC bus voltage. It is compared with the topology proposed at [13].

5.2.1. Short Circuit Fault in Grid Tied Mode

In the grid tied mode short circuit fault is simulated with fault resistance equal to 0.001ohm/Phase at t = 0.1sec.

This fault has been cleared after 0.15seconds. Figure 11 shows the DC bus voltage in the grid tied mode after short circuit fault occurred.

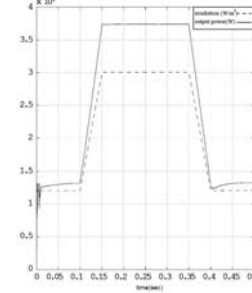


Figure 9. Output power of solar panel versus output voltage.

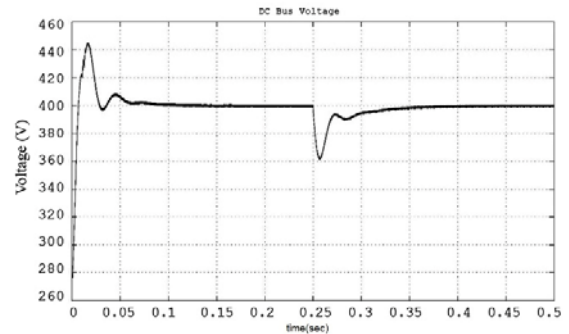


Figure 10. DC bus voltage response (solar irradiation level is fixed at 750 W/m² and DC load increases from 20 kW to 40 kW at t=0.25 sec).

5.2.2. Short Circuit Fault in the Isolated Mode

In the isolated mode fault resistance is 0.00166 ohm/phase and needed time for clearing fault is 0.2 seconds. Figure 12 shows DC bus voltage with short circuit fault at AC side in isolated mode. It is obvious that in isolated mode the recovery time is more than this time in the grid tied mode. Comparison of figures 11 and 12 shows that with same lost energy during faults, DC bus voltage in grid tied mode has smaller overshoot and settling time than that amount in isolated mode, so microgrid in grid tied mode is more stable than isolated mode. In this controller the voltage recovers to 1st value (400V) only after 0.2 seconds in isolated mode and in the grid tied mode this time decrease to 0.15 seconds. But in [13] this time is 2 seconds for isolated mode because in [13] the voltage is supported by synchronous generator lonely but in this paper the main controller supports the voltage in isolated mode and fault clearing time reduces. This shows advantage of the proposed control method introduced in [11].The short circuit fault in both modes have equal lost energy (51 joules).

6. CONCLUSION

An investigation on the Hybrid AC-DC micro grid proposed by Liu, X. et al has been executed. P&O Algorithms for obtaining maximum power from renewable-energy resources and trading power between DC and AC sides were used. Using of hybrid AC-DC microgrid can reduce number of converters and cost, and also can improve stability of the power network. Voltage stability of the DC bus under short circuit fault that

simulated in MATLAB/SIMULINK confirmed that grid tied mode is more stable than isolated mode and the coordination control used is far better than control method proposed by Jayawardena, A. V. et al.

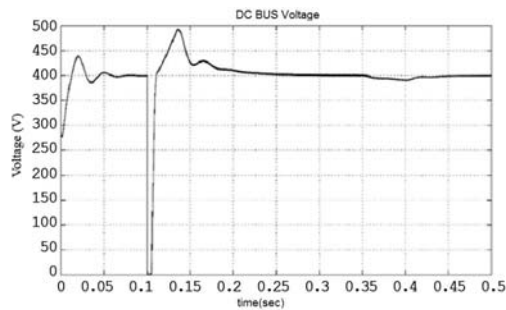


Figure 11. DC bus voltage response in grid tied mode (short circuit fault occurred at 0.1sec).

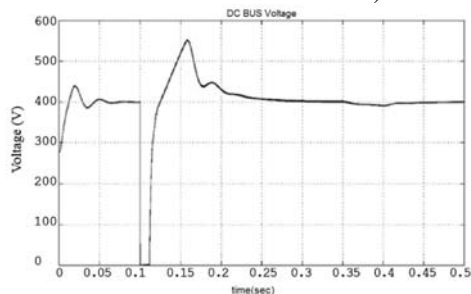


Figure 12. DC bus voltage response in isolated mode (short circuit fault occurred at 0.1sec).

REFERENCES

- [1] Vahidi, B. Jannati, M. Hosseini, S. H. "A novel approach to adaptive single phase autoreclosure scheme for EHV power transmission lines based on learning error function or ADALINE ", *Simulation*, **84**(12): 601-610 (2008).
- [2] Jazebi, S. Hosseini, S. H. Vahidi, B. "DSTATCOM allocation in distribution networks considering reconfiguration using differential evolution algorithm", *Energy Conversion and Management*, **52**(7): 2777-2783 (2011).
- [3] Vahidi, B. Ghafarzadeh, N. Hosseini S. H. "A wavelet-based method to discriminate internal faults from inrush currents using correlation coefficient", *International Journal of Electrical Power & Energy Systems*, **32**(7): 788-793 (2010).
- [4] Bank Tavakoli, M. R. Vahidi, B. "Shielding failure rate calculation by means of downward and upward lightning leader movement models: effect of environmental conditions", *Journal of Electrostatics*, **68**(3): 275-283 (2010).
- [5] Jazebi, S. Vahidi, B. Hosseini, S. H. "A novel discriminative approach based on hidden Markov models and wavelet transform to transformer protection", *Simulation*, **86**(2): 93-107 (2010).
- [6] Vahidi, B. Haghani Abandansari, A. "Teaching ferroresonance in power system to underground students by using Matlab-Simulink", *Computer Applications in Engineering Education*, **19**(2): 347-357 (2011).
- [7] Jazebi, S. Vahidi, B. Hosseini, S. H. "A new stochastic method based on hidden Markov models to transformer differential protection", 11th international conference on optimization of electrical and electronic equipment, OPTIM 2008, pp. 179-184, (2008).
- [8] Justo, J. J. et al. "AC-microgrids versus DC-microgrids with distributed energy resources: A review", *Renewable and Sustainable Energy Reviews*, **24**: 387-405 (2013).
- [9] Ito, Y. Zhongqing, Y. Akagi, H. "DC microgrid based distribution power generation system", 4th International Power Electronics and Motion Control Conference, IPERC 2004, **3**: 1740-1745 (2004).
- [10] Hammerstrom, D. J. "AC versus DC distribution systems did we get it right?", IEEE Power Engineering Society General Meeting, pp. 1-5 (2007).
- [11] Liu, X. Wang, P. Chiang Loh, P. "A hybrid AC/DC micro-grid", IEEE IPEC 2010 Conference Proceedings, pp. 746-751 (2010).
- [12] Mahmudicherati, S. Elbuluk, M. Sozer, Y. "An improved direct power control of a doubly fed induction generator wind power system", IEEE Industry Applications Society Annual Meeting, pp. 1-8 (2013).
- [13] Jayawardena, A. V. et al. "Dynamic characteristics of a hybrid microgrid with inverter and non-inverter interfaced renewable energy sources: A case study" IEEE International Conference on Power System Technology (POWERCON), pp. 1-6 (2012).
- [14] Liu, X., Wang, P. Chiang Loh, P. "A hybrid AC/DC microgrid and its coordination control", *IEEE Transactions on Smart Grid*, **2**(2): 278-286 (2011).
- [15] Dawei, Z. Lie, X. "Direct power control of DFIG with constant switching frequency and improved transient performance", *IEEE Transactions on Energy Conversion*, **22**(1): 110-118 (2007).
- [16] Ropp, M. E. Gonzalez, S. "Development of a MATLAB/Simulink model of a single-phase grid-connected photovoltaic system", *IEEE Transactions on Energy Conversion*, **24**(1): 195-202 (2009).
- [17] Chao, K. H. Li, C. J. Ho, S. H. "Modeling and fault simulation of photovoltaic generation systems using circuit-based model", IEEE International Conference on Sustainable Energy Technologies (ICSET), pp. 290-294 (2008).
- [18] Mazloomzadeh, A. Farhadi, M. Osama, A. M. "Hardware implementation of hybrid AC-DC power system laboratory involving renewable energy sources", 120th ASEE Annual Conference and Exposition, American Society for Engineering Education, pp. 1-14 (2013).
- [19] Liu, F. et al. "A variable step size INC MPPT method for PV systems." *IEEE Transactions on Industrial Electronics*, **55**(7): 2622-2628 (2008).